CARBON 50 (2012) 4252–4258

Available at www.sciencedirect.com

SciVerse ScienceDirect

journal homepage: www.elsevier.com/locate/carbon

The origin of sub-bands in the Raman D-band of graphene

Zhiqiang Luo [a], *Chunxiao Cong* [a], *Jun Zhang* [a], *Qihua Xiong* [a], *Ting Yu* [a,b,c,*]

[a] *Division of Physics and Applied Physics, School of Physical and Mathematical Sciences, Nanyang Technological University, Singapore 637371, Singapore*

[b] *Department of Physics, Faculty of Science, National University of Singapore, Singapore 117542, Singapore*

[c] *Graphene Research Centre, National University of Singapore, Singapore 117542, Singapore*

ARTICLE INFO

Article history:
Received 27 March 2012
Accepted 6 May 2012
Available online 14 May 2012

ABSTRACT

In Raman spectroscopy investigations of defective suspended graphene, splitting in the D band is observed. Four double resonance Raman scattering processes: the outer and inner scattering processes, as well as the scattering processes with electrons first scattered by phonons ("phonon-first") or by defects ("defect-first"), are found to be responsible for these features of the D band. The D sub-bands associated with the outer and inner processes merge with increasing defect concentration. However a Stokes/anti-Stokes Raman study indicates that the splitting of the D band due to the separate "phonon-first" and "defect-first" processes is valid for suspended graphene. For graphene samples on a SiO_2/Si substrate, the sub-bands of D band merge due to the increased Raman broadening parameter resulting from the substrate doping. Moreover, the merging of the sub-bands shows excitation energy dependence, which can be understood by considering the energy dependent lifetime and/or scattering rate of photo-excited carriers in the Raman scattering process.

1. Introduction

In the emerging research area of graphene, which is a monolayer of graphite showing many novel physical properties, Raman spectroscopy has been successfully developed as a quick metrology for identification of single layer feature and edge orientation, evaluation of strain effect and doping concentration, as well as probing of electron–phonon interaction [1–5]. On the other hand, graphene with the unique and simple band structure offers a great opportunity to make clear of the detailed scattering processes of Raman bands in graphitic materials [6–8]. Two dominant characteristic Raman features, the so called G band and G′ (or 2D) band, present in a Raman spectrum of graphene [9,10]. The G band originates from a single resonance process associated with doubly degenerate iTO and LO phonon modes at the Brillouin zone center, while G′ band is associated with two phonon intervalley double resonance (DR) scattering involving iTO phonon near the *K* point [9]. In defective graphene, a defect induced D band, which originates from a DR Raman process involving intervalley scattering of iTO phonon near the *K* point, appears around the G band [10]. Due to the DR nature, the D band and G′ band of graphene show great importance in not only the Raman spectroscopy but also the electronic structure study of graphene [9]. It is widely accepted that the D band and G′ band, are composed of a single and symmetric Lorentzian peak for single layer graphene [9–12]. However, the theoretical calculation of the D/G′ bands of graphene suggested that the D band and G′ band of graphene should be in a split form, since both the outer process in *KΓ* direction and the inner process in *KM* direction should play significant contribution in DR Raman scattering [13]. Recently, the splitting in the G′ band was

* *Corresponding author at:* Division of Physics and Applied Physics, School of Physical and Mathematical Sciences, Nanyang Technological University, Singapore 637371, Singapore.
E-mail address: Yuting@ntu.edu.sg (T. Yu).

0008-6223/$ - see front matter
http://dx.doi.org/10.1016/j.carbon.2012.05.008

reported in deliberate peak fitting [14,15]. However, the spectral features of the D band have not yet been investigated carefully.

In this contribution, using suspended graphene samples, we revealed the splitting in the D band, and further exploited the Raman scattering processes corresponding to those sub-bands. In addition to the theoretically predicted two individual DR Raman scattering: the outer and inner processes, the coexistence of other two DR Raman scattering processes: electrons first scattered by phonons ("phonon-first") or by defects ("defect-first"), was found to play more important contribution to the splitting of the D band. For graphene samples on a SiO_2/Si substrate, splitting of the D band was also observed but it strongly dependents on the excitation energy, which is caused by the energy dependent lifetime and/or scattering rate of photo-excited carriers in the Raman scattering process. These interesting results would contribute significantly to the understanding of the Raman scattering processes of the D band in graphitic materials.

2. Experimental

Graphene on Si wafer substrate with 285 nm SiO_2 capping layer was prepared by mechanical cleavage from highly ordered pyrolytic graphite (HOPG). The suspended graphene samples were prepared by micromechanical exfoliation of HOPG onto a SiO_2/Si substrate pre-patterned with an array of holes (the diameter of the hole is 3 μm, see the inset of Fig. 1(a)), which was fabricated by photolithography and reactive ion etching [4]. It is worth to point out that the strain effect in graphene have strong influence on the peak features of the D and G′ bands [14]. The suspended graphene samples without significant strain were chose for this experiment. Actually, the strain effect in our suspended graphene is very weak, which was carefully studied in our previous report [4]. For introduction of defects in graphene, the graphene samples were hydrogenated via hydrogen plasma [16]. Adsorption of hydrogen atoms on graphene results in the formation of sp^3 C–H bonds, which are defects in the sp^2 C = C network

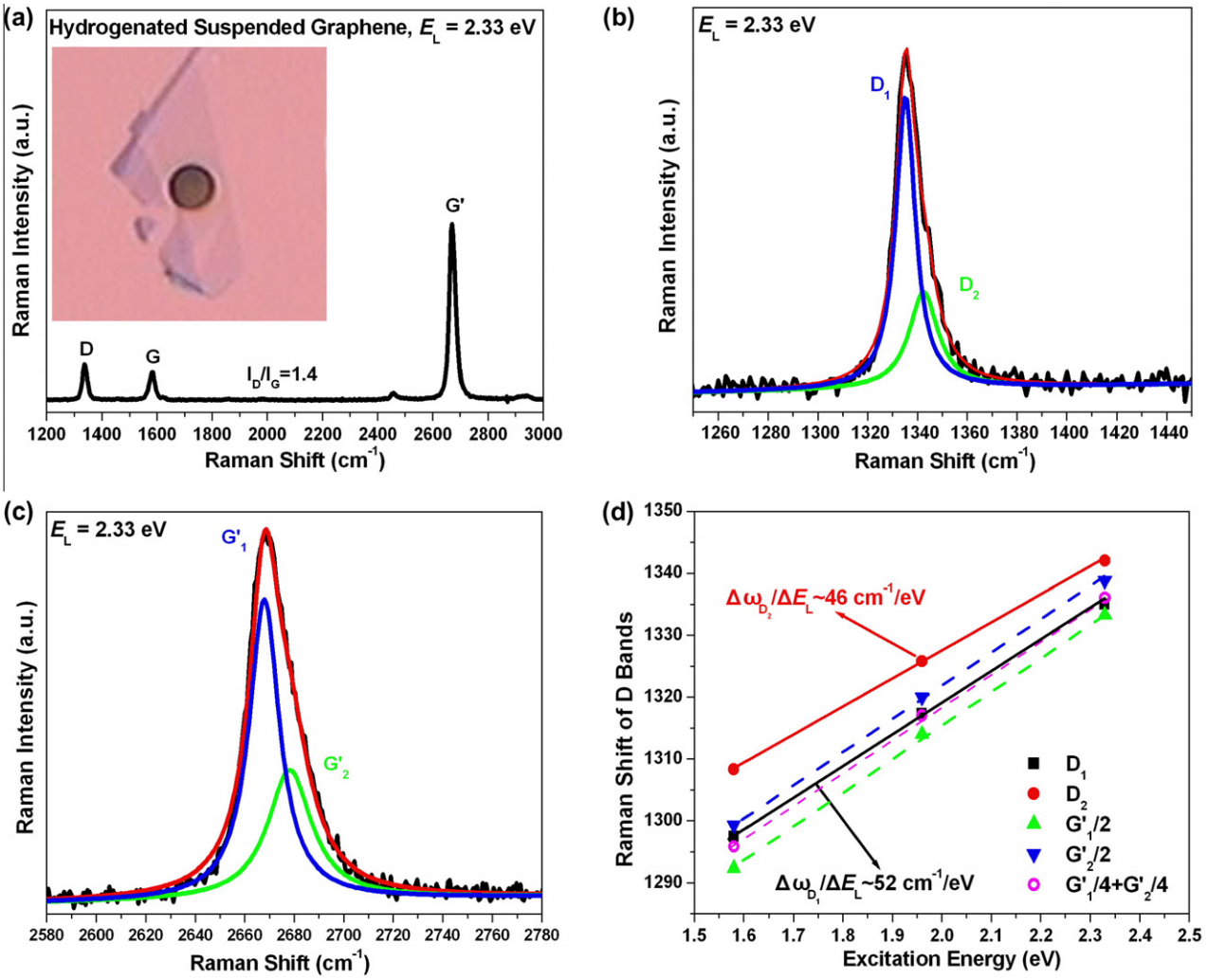

Fig. 1 – (a) Raman spectrum of the suspended graphene after introduction of defects by hydrogenation. The excitation energy is 2.33 eV. The insert is the optical image of a suspended graphene. (b) Lorentzian fitting of the D band of the suspended graphene. (c) Lorentzian fitting of the G′ band of the suspended graphene. (d) Energy dispersion of the D and G′ sub-bands.

[16]. The defect concentration, i.e. the coverage of hydrogen atoms, can be monitored by the intensity ratio of the D band to G band (I_D/I_G) and adjusted by modulating hydrogen plasma treatment dose [16–18]. The Raman spectra were recorded by Renishaw inVia Raman system with excitation lasers of 2.33 eV (532 nm) and 1.58 eV (785 nm), and Jonin-Yvon T64000 Raman system with excitation laser of 1.96 eV (633 nm). The laser power on graphene sample is kept below 1 mW to avoid possible laser-induced heating.

3. Results and discussion

Fig. 1(a) shows a Raman spectrum of hydrogenated suspended graphene, which displays the sharp D, G, and G′ bands. The Lorentzian peak fittings of the D and G′ bands show that these two Raman peaks are highly asymmetric and can be fitted by two Lorentzian components (see Fig. 1(b) and (c)). The splitting of G′ band had been theoretically predicted and experimentally observed [13,14]. Our recent polarized Raman spectroscopy study of the suspended graphene confirmed that the G'_1 at lower frequency and G'_2 at higher frequency should be assigned to outer process and the inner process, respectively [15]. Since the G′ band is the overtone of the D band [9], it would be reasonable to associate the D_1 at lower frequency and D_2 at higher frequency with the G'_1 and G'_2 sub-bands and attribute the origin of splitting in the D band to the coexistence of the outer and inner processes in DR scattering. However, as shown in Fig. 1(d), the energy dependence of D_1, D_2, $G'_1/2$, and $G'_2/2$ do not support this assumption. The energy dependence of the D_1 band is about 52 cm^{-1}/eV, which is close to those of the $G'_1/2$ and G′/2. The energy dependence of the D_2 band has a smaller value, 46 cm^{-1}/eV. The frequency of D_1 (ω_{D1}) matches well with the value of $\omega' = [(\omega_{G'1}/2) + (\omega_{G'2}/2)]/2$, while the frequency of D_2 (ω_{D2}) has a much larger value than those of the ω', $\omega_{G'1}/2$, and $\omega_{G'2}/2$. Therefore, the D_1 band should have strong relationship with the G'_1 and G'_2 band, whereas the origin of the D_2 band should not result from the outer or inner processes mentioned above.

Different from the DR Raman scattering process associated with the G′ band, which involves inelastic scattering of electrons by two phonons, the DR Raman scattering process associated with the D band consists of one inelastic scattering of electron by a phonon and one elastic scattering of electron by a defect [9,10]. In addition to the outer and inner scattering processes in DR Raman scattering, there are two more types of scattering processes for the D band. As illustrated in Fig. 2, in the outer process of the D band, the photo-excited electrons can be first scattered by a phonon or by a defect, which result in distinguishable difference in the frequency of the D band [19]. For example, in Stokes Raman scattering of the D band, the change in electron momentum is larger when the electron is first scattered by a defect, which involves a phonon with larger frequency. These two different scattering processes would be responsible for our observed splitting of D band. It would be appropriate to mark the D_1 and D_2 in Fig. 1 to "phonon-first" and "defect-first" processes, respectively. The "phonon-first" process of the D band is actually similar to the first half part of the scattering process of the G′ band [9]. The observed D_1 sub-band should be a merged

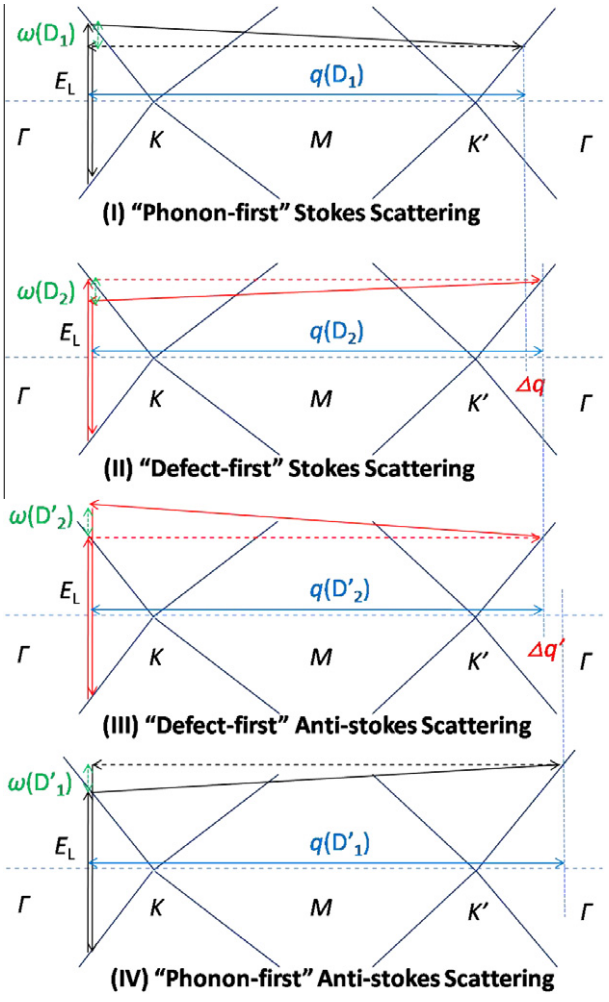

Fig. 2 – The illustration of "phonon-first" and "defect-first" processes in Stokes and anti-Stokes outer processes of the D band.

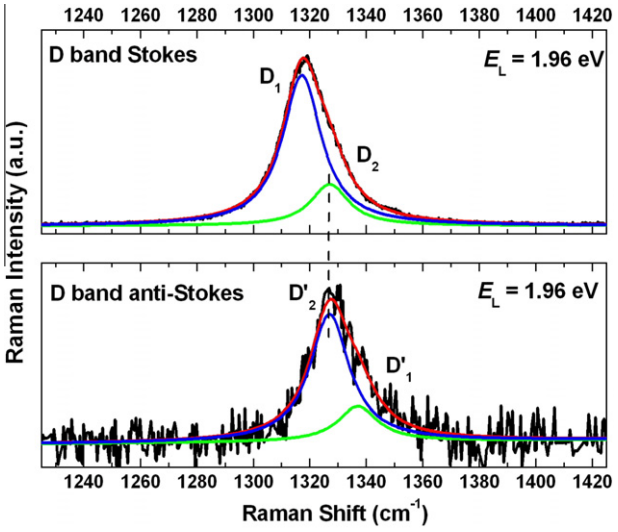

Fig. 3 – Stokes and anti-Stokes Raman spectra of the D band. (The excitation energy is 1.96 eV).

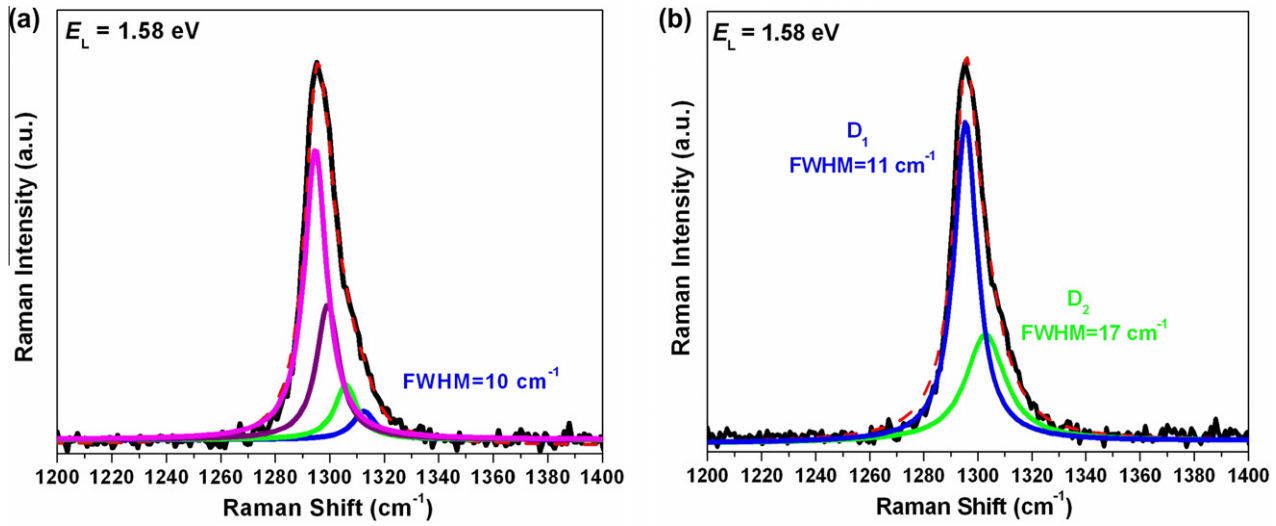

Fig. 4 – (a) Fitting of the D band (excited by 1.58 eV) with four Lorentzian lines corresponding to the "phonon-first"-outer, "phonon-first"-inner, "defect-first"-outer, and "defect-first"-inner processes. (b) Fitting of the same D band with two Lorentzian lines. (Under the excitation energy of 2.33 eV, the I_D/I_G of this suspended graphene sample is 0.1).

peak of the outer and inner component within the "phonon-first" process of the D band. Therefore, it is reasonable that ω_{D1} is close to $[(\omega_{G'1}/2) + (\omega_{G'2}/2)]/2$.

A strong evidence supporting the interpretation with the above mentioned "phonon-first" and "defect-first" processes comes from the study of Stokes and anti-Stokes Raman scattering of the D band. As illustrated in Fig. 2, for the "defect-first" process, the frequency of Stokes scattering (ω_{D2}) is the same as the frequency of anti-Stokes scattering ($\omega_{D'2}$). For the "phonon-first" process, the frequency of the Stokes scattering (ω_{D1}) is smaller than ω_{D2}. However, in anti-Stokes scattering, $\omega_{D'1}$ becomes larger than $\omega_{D'2}$. This theoretical picture is consistent with our experimental observation shown in Fig. 3 (in order to obtain strong D band anti-Stokes Raman scattering signal, the I_D/I_G of this suspended sample is as large as three under the excitation of 2.33 eV). Under the excitation of 1.96 eV, the frequencies of the "defect-first" processes for Stokes and anti-Stokes scattering are the same ($\omega_{D2} = \omega_{D'2} = 1327\ cm^{-1}$). The frequencies of the "phonon-first" processes for Stokes and anti-Stokes scattering are 1317 and 1337 cm^{-1}, respectively, which are in good agreement with the illustration in Fig. 2.

It should be point out that the "phonon-first" or "defect-first" process each contains the outer and inner processes, and thus in theory there should be four sub-bands in each D band. Due to defect induced broadening of the full width at half-maximum (FWHM) of D sub-bands [12,18], the D sub-bands associated with the outer and inner processes may merge, which is evidenced by $\omega_{D1} \approx \omega' = [(\omega_{G'1}/2) + (\omega_{G'2}/2)]/2$ (see Fig. 1 (d)). When the defect concentration is ultra low ($I_D/I_G = 0.1$ under the excitation of 2.33 eV), the D band excited by near infrared (NIR, 1.58 eV) laser can be carefully

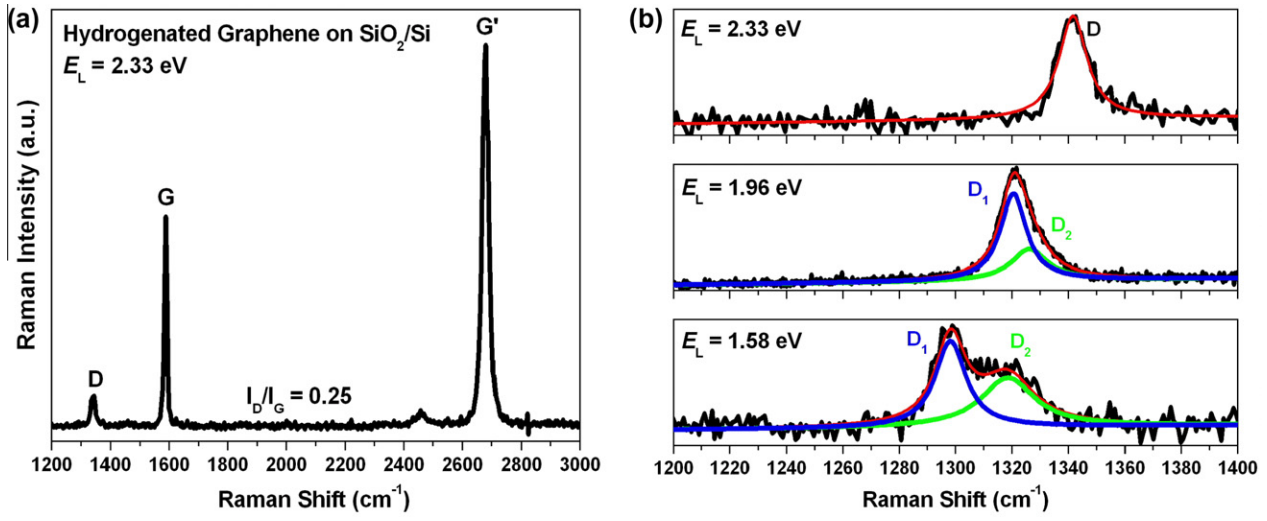

Fig. 5 – (a) Raman spectrum of hydrogenated graphene on a SiO_2/Si substrate (excitation energy is 2.33 eV). (b) Lorentzian fittings of the D bands excited by 2.33, 1.96, and 1.58 eV lasers.

fitted with four Lorentzian lines (shown in Fig. 4(a)). Actually, when the D band was fitted with two Lorentzian lines (see Fig. 4(b)), the deviation of FWHM of the two D sub-bands is significant. In this case, the defect induced FWHM broadening of D sub-bands should not be significant. Therefore, all the four DR scattering processes, including the "phonon-first"-outer process, "phonon-first"-inner process, "defect-first"-outer process, "defect-first"-inner process, are responsible for the peak features of the D band. However, the "phonon-first" and "defect-first" processes are the main origin of the observed splitting of the D band in Fig. 1, which is associated with a much higher defect concentration (I_D/I_G = 1.4).

For suspended graphene samples with different defect concentration (under the excitation of 2.33 eV, I_D/I_G varies from 0.1 to 5), the sub-bands can always be fitted out in D band excited by all the excitation energies. However, for graphene samples on a SiO_2/Si substrate, the sub-bands of D band are hardly being resolved, suggesting the weak doing effect induced by SiO_2/Si substrate plays significant influence on the merging of the D sub-bands [20]. The weak doping effect from the SiO_2 substrates in our samples is evidenced by an obvious blue shift of G band from 1582 (suspended graphene) to 1588 cm^{-1} (graphene on SiO_2) and the strongly decreased $I_{G'}/I_G$ ratio (see Figs. 1 and 5(a)) [4]. Interestingly, it has been note that the single Lorentzian line fitting of D band of graphene on a SiO_2/Si substrate is not valid all the time. Fig. 5(a) demonstrates a Raman spectrum of hydrogenated graphene under the excitation of 2.33 eV. The D band excited by 2.33 eV laser seems symmetric, and its single Lorentzian peak fitting is shown in the upper panel of Fig. 5(b). Whereas, under the excitation of 1.96 eV, the D band becomes asymmetric obviously. The asymmetric feature became more pronounced under the excitation of 1.58 eV, which has to be fitted by two Lorentzian lines. Such excitation energy dependent splitting of the D band can be observed in graphene samples with a wide range of defect concentrations. As shown in

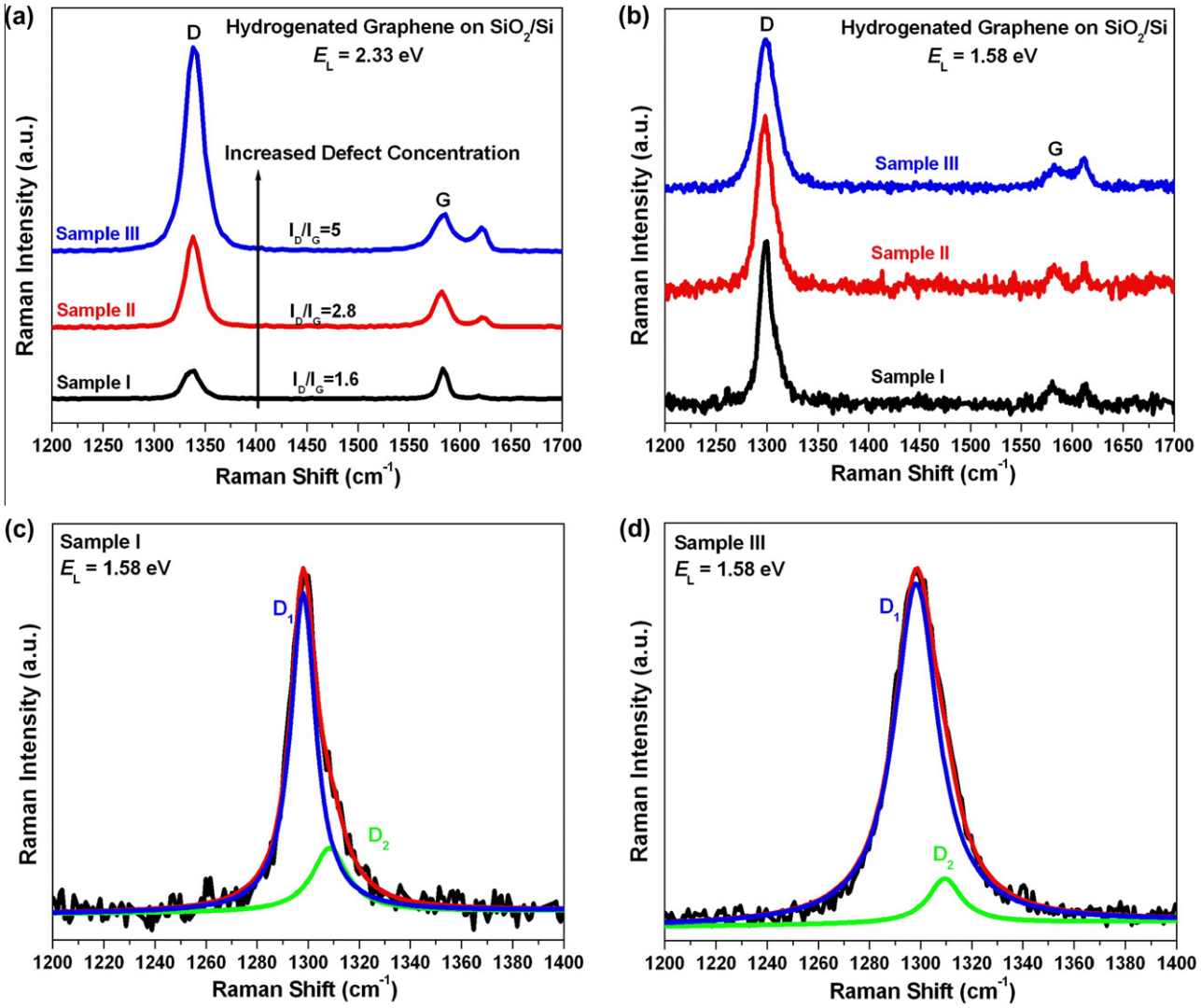

Fig. 6 – (a) Raman spectra of hydrogenated graphene on a SiO_2/Si substrate (the excitation energy is 2.33 eV); (b) Raman spectra recorded under 1.58 eV excitation for the same samples listed in (a); (c) (d) Lorentzian fittings of the D bands shown in (b).

Fig. 6, all the D bands under the excitation of 2.33 eV seem symmetric, while they become asymmetric obviously under the excitation of 1.58 eV.

This excitation energy dependent splitting phenomenon can be understood by considering the energy depended lifetime (τ) and/or scattering rate ($1/\tau$) of photo-excited carriers. The Raman cross section of the D band can be represented as,

$$PK_{2f,10} = \sum_{a,b,c} \frac{M_{fc}M_{cb}M_{ba}M_{ai}}{(E_l - E_{ai} - i\hbar\gamma)(E_l - \hbar\omega - E_{bi} - i\hbar\gamma)(E_l - \hbar\omega - E_{ci} - i\hbar\gamma)} + \frac{M_{fc}M_{cb}M_{ba}M_{ai}}{(E_l - E_{ai} - i\hbar\gamma)(E_l - \hbar\omega - E_{bi} - i\hbar\gamma)(E_l - \hbar\omega - E_{ci} - i\hbar\gamma)}$$

where M_{xy} is the matrix element for the scattering over the intermediate states x and y, E_l and E_l -$\hbar\omega$ are the energies of the incoming and outgoing photon, and γ is the broadening parameter of the electronic transition [13]. The theoretical calculation based on the above formula indicates that large broadening parameter of the electronic transition would cause significant electron broadening in DR Raman scattering process of the D band and therefore merging of the sub-bands [13]. In a Raman resonance scattering process, the broadening parameter of the electronic transition, γ, is proportional to the scattering rate ($1/\tau$) of the photo-excited carriers [21]. On basis of the linear dispersion in graphene, the energy of a photo-excited carrier, $E = E_L/2$, where E_L is the excitation energy of a laser. There are mainly three decay channels for these excited carriers, electron–phonon scattering via electron–phonon interaction, as well as electron–electron scattering (generation of electron–hole pairs) and electron-plasmon scattering (excitation of plasmonic mode) via electron–electron interaction [22,23]. Both the theoretical calculation and experimental results from the angle resolved photoemission spectroscopy measurements indicate that the electron–phonon interaction and electron–electron interaction in graphene have comparable contribution to the decay of photo-excited carriers [22–24]. In comparison to the suspended graphene, graphene on a SiO_2/Si substrate is p-doped with an excess carrier density [4,20]. The scattering rate of photo-excited carriers subject to electron–electron interaction ($1/\tau_{e\text{-}e}$ and $1/\tau_{e\text{-}p}$) shows strong dependence on carrier density [25]. Therefore, for graphene on a SiO_2/Si substrate, the contribution to the broadening parameter from the electron–electron interaction should be enhanced. Moreover, the scattering rate of photo-excited carriers subject to the electron–electron scattering ($1/\tau_{e\text{-}e}$) and electron-plasmon scattering ($1/\tau_{e\text{-}p}$) are proportional to $(E\text{-}E_F)^2$ and $(E\text{-}E_F)$, respectively, where E_F is the Fermi level [26]. It is clear that the scattering rates show energy dependence, and smaller excitation energy will result in smaller broadening parameter in the Raman resonance scattering. Thus, in the presence of substrate doping, the merging degree of the D sub-bands is lower at smaller excitation energy, and the splitting of the D band looks more apparent, as displayed in Fig. 5(b).

4. Conclusions

There are four DR scattering processes, including the "phonon-first"-outer process, "phonon-first"-inner process, "defect-first"-outer process, "defect-first"-inner process, responsible for the peak features of the D band. The defect induced broadening of FWHM of the D sub-bands results in merging of the D sub-bands associated with the outer and inner processes. However, the splitting of the D band due to the separate "phonon-first" and "defect-first" processes is valid for suspended graphene, which is supported by a Stokes/anti-Stokes Raman spectroscopy study of the D band. For graphene samples on a SiO_2/Si substrate, the D band shows an asymmetric peak under NIR excitations, while it becomes symmetric peak under higher energy excitations. This excitation energy depended splitting can be explained by the energy dependent lifetime and/or scattering rate of photo-excited carriers in the Raman scattering process. This careful study in the D band of graphene contributes significantly to the understanding of the detailed Raman scattering processes of the D band in graphitic materials.

Acknowledgements

The work is funded by the Singapore National Research Foundation under NRF RF Award No. NRF-RF2010-07 and MOE Tier 2 MOE2009-T2-1-037.

REFERENCE

[1] Ferrari AC, Meyer JC, Scardaci V, Casiraghi C, Lazzeri M, Mauri F, et al. Raman spectrum of graphene and graphene layers. Phys. Rev. Lett. 2006;97:187401.
[2] Cong C, Yu T, Wang H. Raman study on the G mode of graphene for determination of edge orientation. ACS Nano 2010;4:3175–80.
[3] Yu T, Ni Z, Du C, You Y, Wang Y, Shen ZX. Raman mapping investigation of graphene on transparent flexible substrate: the strain effect. J. Phys. Chem. C 2008;112:12602–5.
[4] Ni ZH, Yu T, Luo ZQ, Wang Y, Liu L, Wong CP, et al. Probing charge impurities in suspended graphene by Raman spectroscopy. ACS Nano 2009;3:569–74.
[5] Pisana S, Lazzeri M, Casiraghi C, Novoselov KS, Geim AK, Ferrari AC, et al. Breakdown of the adiabatic Born-Oppenheimer approximation in graphene. Nature Mater. 2007;6:198–201.
[6] Yoon D, Moon H, Son YW, Samsonidze G, Park BH, Kim JB, et al. Strong polarization dependence of double-resonant raman intensities in graphene. Nano Lett. 2008;12:4270–4.
[7] Beams R, Cançado LG, Novotny L. Low temperature raman study of the electron coherence length near graphene edges. Nano Lett. 2011;11:1177–81.
[8] Rao R, Tishler D, Katoch J, Ishigami M. Multiphonon Raman scattering in graphene. Phys. Rev. B 2011;84:113406.
[9] Malard LM, Pimenta MA, Dresselhaus G, Dresselhaus MS. Raman spectroscopy in graphene. Phys. Rep. 2009;473:51–87.
[10] Ferrari AC. Raman spectroscopy of graphene and graphite: disorder, electron–phonon coupling, doping and nonadiabatic effects. Solid State Commun. 2007;143:47–57.
[11] Ni ZH, Wang Y, Yu T, Shen ZX. Raman spectroscopy and imaging of graphene. Nano Res. 2008;1:273–91.
[12] Ferreira EHM, Moutinho MVO, Stavale F, Lucchese MM, Capaz RB, Achete CA. Evolution of the Raman spectra from single-, few-, and many-layer graphene with increasing disorder. Phys. Rev. B 2010;82:125429.
[13] Mohr M, Maultzsch J, Thomsen C. Splitting of the Raman 2D band of graphene subjected to strain. Phys. Rev. B 2010;82:201409(R).

[14] Frank O, Mohr M, Maultzsch J, Thomsen C, Riaz I, Jalil R, et al. Raman 2D-band splitting in graphene: theory and experiment. ACS Nano 2011;5:2231–9.
[15] Luo ZQ, Cong CX, Zhang J, Xiong QH, Yu T. Direct observation of inner and outer g′ band double-resonance raman scattering in free standing graphene. arXiv:1204.6356.
[16] Luo ZQ, Yu T, Kim KJ, Ni ZH, You YM, Lim SH, et al. Thickness-dependent reversible hydrogenation of graphene layers. ACS Nano 2009;3:1781–8.
[17] Luo ZQ, Shang JZ, Lim SH, Li DH, Xiong QH, Shen ZX, et al. Modulating the electronic structure of graphene by controllable hydrogenation. Appl. Phys. Lett. 2010;97:233111.
[18] Luo ZQ, Yu T, Ni ZH, Lim SH, Hu HL, Shang JZ, et al. Electronic structures and structural evolution of hydrogenated graphene probed by Raman spectroscopy. J. Phys. Chem. C 2011;115:1422–7.
[19] Cancado LG, Pimenta MA, Saito R, Jorio A, Ladeira LO, Grueneis A, et al. Stokes and anti-Stokes double resonance Raman scattering in two-dimensional graphite. Phys. Rev. B 2002;66:035415.
[20] Casiraghi C. Doping dependence of the Raman peaks intensity of graphene close to the Dirac point. Phys. Rev. B 2009;80:233407.
[21] Park JS, Oyama Y, Saito R, Izumida W, Jiang J, Sato K, et al. Raman resonance window of single-wall carbon nanotubes. Phys. Rev. B 2006;74:165414.
[22] Bostwick A, Ohta T, Seyller T, Horn K, Rotenberg E. Quasiparticle dynamics in graphene. Nature Phys. 2007;3:36–40.
[23] Park CH, Giustino F, Spataru CD, Cohen ML, Louie SG. First-principles study of electron linewidths in graphene. Phys. Rev. Lett. 2009;102:076803.
[24] Sugawara K, Sato T, Souma S, Takahashi T, Suematsu H. Anomalous quasiparticle lifetime and strong electron–phonon coupling in graphite. Phys. Rev. Lett. 2007;98:036801.
[25] Basko DM, Piscanec S, Ferrari AC. Electron-electron interactions and doping dependence of the two-phonon Raman intensity in graphene. Phys. Rev. B 2009;80:165413.
[26] Xu S, Cao J, Miller CC, Mantell DA, Miller RJD, Gao Y. Energy dependence of electron lifetime in graphite observed with femtosecond photoemission spectroscopy. Phys. Rev. Lett. 1996;76:483–6.